NASA Contractor Report 3583

Simulation of a Hydrocarbon Fueled Scramjet Exhaust

Jarvis Leng

CONTRACT NAS1-16401
JUNE 1982

NASA

NASA Contractor Report 3583

Simulation of a Hydrocarbon Fueled Scramjet Exhaust

Jarvis Leng
Grumman Aerospace Corporation
Bethpage, New York

Prepared for
Langley Research Center
under Contract NAS1-16401

National Aeronautics
and Space Administration

Scientific and Technical
Information Office

1982

TABLE OF CONTENTS

LIST OF ILLUSTRATIONS

LIST OF TABLES

SYMBOLS

A	area
Ar	argon atom
a	sound speed
Br	bromine atom
C	carbon atom
CTF	chlorine trifluoride
Cl	chlorine atom
c_p	specific heat at constant pressure
c_v	specific heat at constant volume
c	prefix "centi" (10^{-2})
F	fluorine atom; also force per unit width
Freon 13B1	bromotrifluoromethane ($CBrF_3$)
H	enthalpy; also hydrogen atom
K	Kelvin temperature scale
k	prefix "kilo" (10^3)
M	Mach number ($\equiv$ U/a)
MOC	method of characteristics
m	unit of length (meter)
N	nitrogen atom
O	oxygen atom
P	pressure
T	temperature
U	velocity

X,x	distance measured along combustor axis (vehicle roll axis)
$\overline{X}$	nondimensional distance ($\equiv X/Y_e$)
Y	vehicle yaw axis
$\overline{Y}$	nondimensional distance ($\equiv Y/Y_e$)
α	angle of attack
γ	ratio of specific heats, c_p/c_v
θ	flow angle relative to X axis
ρ	density

Subscripts

o	refers to total (stagnation) condition
e	refers to combustor exit plane
H	horizontal (in X direction)
v	vertical (in Y direction)
∞	refers to undisturbed free stream

1. INTRODUCTION

This report presents an analysis of substitute gases for use in simulating exhaust flows of hydrocarbon-fueled scramjets. The concept of a fully-integrated supersonic combustion ramjet has been developed in a series of investigations centered at NASA Langley Research Center (Refs. 1 and 2). A fully integrated scramjet is one that employs the entire windward surface of the forebody in the inlet compression process and the entire windward surface of the afterbody in the exhaust expansion process. Such a vehicle is depicted schematically in Fig. 1. It offers a minimum weight method of maximum utilization for propulsive purposes of air that has been compressed by the windward forebody shock wave, thus maximizing net thrust. At the same time, it raises the problem of engine/ airframe integration to a new level of importance. Foremost among the aerodynamic issues of such a vehicle is the sensitivity of forces and moments to the thermodynamic behavior of the hot scramjet exhaust as it expands over the afterbody/nozzle. The exhaust gases are very much hotter than the ambient flow, and contain products of combustion that, together with the higher temperature, produce a significantly lower ratio of specific heats (γ) than exists in the ambient. In the expanding exhaust flow, this lower γ results in a local normal force on the afterbody that can be ten times what it would be if the exhaust were low temperature air at $\gamma = 1.4$ (Ref. 3). Prediction of the approximate range of these forces is a relatively easy task with modern computational methods, but the aerodynamic development of such vehicles in hypersonic wind tunnels presents a much more difficult problem.

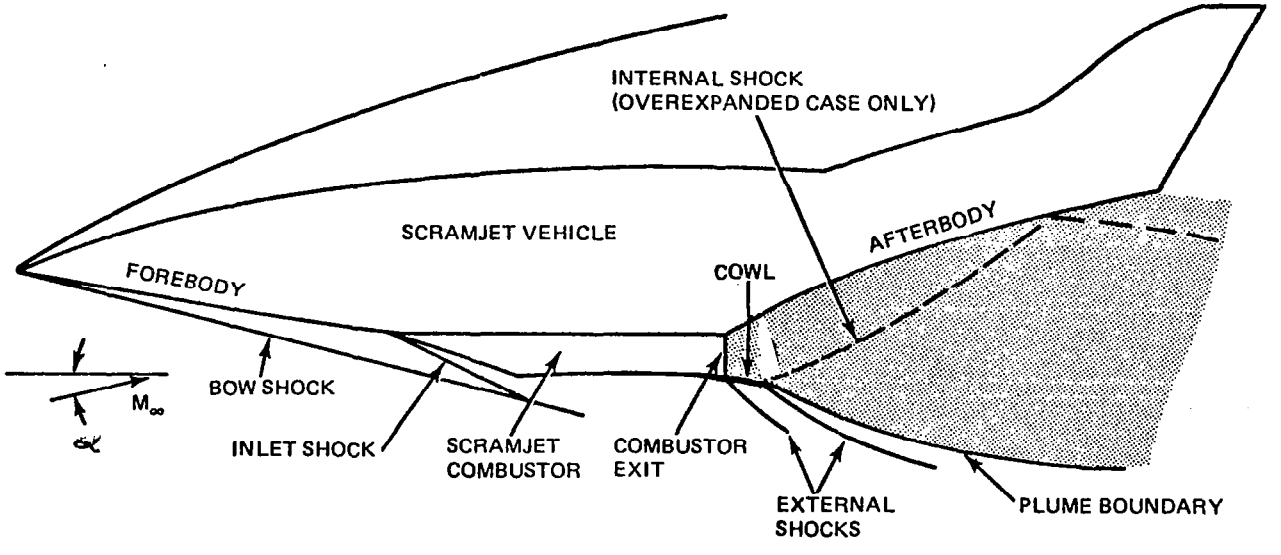

Fig. 1 Schematic Drawing of Typical Scramjet Vehicle

In a series of investigations that took place in the mid 1970's (Refs. 3-5), Grumman Aerospace Corporation addressed the problem of properly integrating the exhaust flow of a hydrogen fueled scramjet into the aerodynamic development of a hypersonic vehicle. The solution was based on the use of a substitute gas that was specifically tailored to provide a cool flow that was fluid dynamically and thermodynamically similar to the actual expanding exhaust gases. This gas was then used as a propulsion-flow medium, injected at appropriate rates through the exhaust nozzles of hypersonic wind tunnel models, so that flow fields could be similar between model and flight prototype. This report describes the definition of such exhaust simulation gases for a hydrocarbon fueled, fully-integrated scramjet vehicle.

The basis for substitute-gas simulation of scramjet exhausts is described in detail in Ref 3. A typical nozzle profile is chosen, and the actual scramjet exhaust flow is calculated using the method of characteristics (MOC). Use of MOC avoids any concern over large errors that might occur in finite difference methods near the origin of the Prandtl-Meyer expansions that are typical in these nozzles. As a practical matter, the MOC is usually run assuming both frozen and equilibrium chemistry, and finite rate chemistry calculations are performed only for those cases for which neither extreme is adequate.

The distribution of the specific heat ratio is the key to the preliminary definition of the correct substitute gas. Mixtures of fluorocarbons (γ very near unity) and argon ($\gamma = 5/3$) are easily formulated to achieve any desired level of γ at a particular point (i.e., temperature) in the flow field. Slightly more difficult is the challenge of finding a blend of fluorcarbon and argon that matches the $\gamma(T/T_{ref})$ behavior of the actual

combustion products over the range of temperature ratio that characterizes the entire nozzle. The range of temperatures employed in the substitute gas is somewhat flexible, but it must be held to the practical limits of the wind tunnel facility in which the final experiments are to be conducted. Finally, the substitute gas and temperature range selected must be run through the MOC program with the actual $\gamma(T)$ behavior of the substitute gas, so that pressure and Mach number distributions can be compared.

2. COMBUSTOR EXHAUST CHEMISTRY

The hydrocarbon fuels of interest for this study consist of blends of Shelldyne* and Chlorine Trifluoride (CTF). Two flight conditions were considered: Mach 4 at 6.1 km altitude (20,000 ft) and Mach 6 at 30.5 km altitude (100,000 ft). At Mach 4 the fuel blend is 80% Shelldyne and 20% CTF (by weight) at a fuel equivalence ratio of 1.0. At Mach 6 the blend is 90% Shelldyne and 10% CTF at an equivalence ratio of 0.7. Since analysis of the scramjet engine combustion process was beyond the scope of the present study, the scramjet combustor exit plane properties were supplied by the NASA/Langley Research Center's Hypersonic Aerodynamic Branch, and are presented in Table 1. Two angles-of-attack were considered for the Mach 6 flight case. From these data the combustor isentropic stagnation conditions were calculated and then tables of isentropic expansion properties

---

* Shelldyne is a synthetic, high-energy, heavy hydrocarbon fuel, sometimes called RJ-5. Approximate formula: $C_{14}H_{18}$; approx. spec. grav. = 1.08 (Ref. 6)

Table 1 Hydrocarbon Scramjet Combustor Exit Flow Properties

	$M_\infty = 4$	$M_\infty = 6$	
	$\alpha = 0°$	$\alpha = 0°$	$\alpha = 6°$
P, atm	2.2418	0.736	0.1079
T, K	1797.9	1717.6	1733.1
H, cal/gm	-250.7	-261.2	-256.1
ρ, gm/cm^3	4.4909-4	1.5407-5	2.2399-5
Mole wt.	29.554	29.520	29.525
γ	1.2465	1.2368	1.2370
a, m/sec	794.0	773.5	777.1
M	2.129	2.728	2.701
Mole Fractions			
Ar	0.00868	0.00876	0.00876
CO	0.00075	0.00161	0.00160
CO_2	0.15028	0.14885	0.14886
Cl	0.00009	0.00007	0.00007
H	--	0.00001	0.00001
HCl	0.00536	0.00234	0.00235
HF	0.01633	0.00723	0.00723
H_2	0.00012	0.00029	0.00029
H_2O	0.08809	0.09356	0.09356
NO	0.00025	0.00020	0.00021
N_2	0.72922	0.73608	0.73609
O	--	0.00001	0.00001
OH	0.00012	0.00018	0.00018
O_2	0.00071	0.00080	0.00079

determined by the computer program of Ref. 7, for both equilibrium flow and flow chemically frozen at the combustor exit plane. (The calculation of isentropic stagnation conditions is a necessary intermediate step in producing tables of thermodynamic expansion products and does not imply the actual flow stagnates. In a scramjet combustor the flow is everywhere supersonic.)

3. AFTERBODY NOZZLE FLOW FIELDS

The tables of thermodynamic flow properties are used in conjunction with the method-of-characteristics (MOC) computer program of Ref. 8 to calculate the two-dimensional afterbody nozzle flow fields. The nozzle geometry chosen to analyze was identical to that used in a previous study (Ref. 5), namely a 20° expansion nozzle with a cowl with a 6° expansion angle. No shock waves were considered in these calculations. The geometry of the afterbody and cowl are given below.

Cowl

$\bar{Y} = 1.0$	$0 < \bar{X} < 1.11$
$\bar{Y} = 0.4204\ \bar{X}^2 - 0.933\ \bar{X} + 1.518$	$1.11 < \bar{X} < 1.235$
$\bar{Y} = 0.1051\ \bar{X} + 0.8768$	$1.235 < \bar{X} < 3.12$

20° Afterbody

$\bar{Y} = (0.1736 - \bar{X}^2)^{1/2} - 0.4167$	$0 < \bar{X} < 0.1425$
$\bar{Y} = -0.3640\ \bar{X} + 0.02674$	$0.1425 < \bar{X} < 21.67$

where $\bar{Y} = Y/Y_e$, $\bar{X} = X/Y_e$, and Y_e is the height of the combustor exit.

Calculations were made for 6 cases: $M_\infty = 4$ and $M_\infty = 6$ at angle-of-attack (α) = 0°, and $M_\infty = 6$ at $\alpha = 6°$, all assuming both equilibrium and frozen chemistry. We found that at a given Mach number there was negligible difference in the flow properties as a function of position between the frozen flow case and the equilibrium flow case. Likewise, there was negligible difference in flow properties between the two angle of attack cases at $M_\infty = 6$, with the exception that the overall pressure levels were higher at the higher angle of attack. There were significant differences in the flow fields at the two different flight Mach numbers and these are illustrated in Figures 2 and 3, which show respectively, the two-dimensional flow fields for the $M_\infty = 4$, $\alpha = 0°$, equilibrium flow case, and the $M_\infty = 6$, $\alpha = 0°$, equilibrium flow case.

The flow fields shown in these figures each have several zones of uniform, constant property flow, which are labeled A, B, C, etc. Table 2 shows the local Mach number, pressure, and flow angularity (θ) in each of these zones which further illustrates the similarties and differences in the flows for the six cases under consideration. Also shown in this Table (for ease of comparison) are the results from some of our substitute gas calculations, which will be discussed in Section 6. Substitute Gases.

4. FINITE-RATE CHEMISTRY EFFECTS

With the frozen flow and equilibrium flow calculations showing negligible differences it would be likely that any effect of finite-rate chemistry should also be negligible. However, it is conceivable in complex chemical systems where both two-body and three-body collisions take place, that one group of reactions may occur much more rapidly than another group, and that this might produce a thermodynamic path outside the bounds of completely frozen and completely equilibrium processes. To examine this point

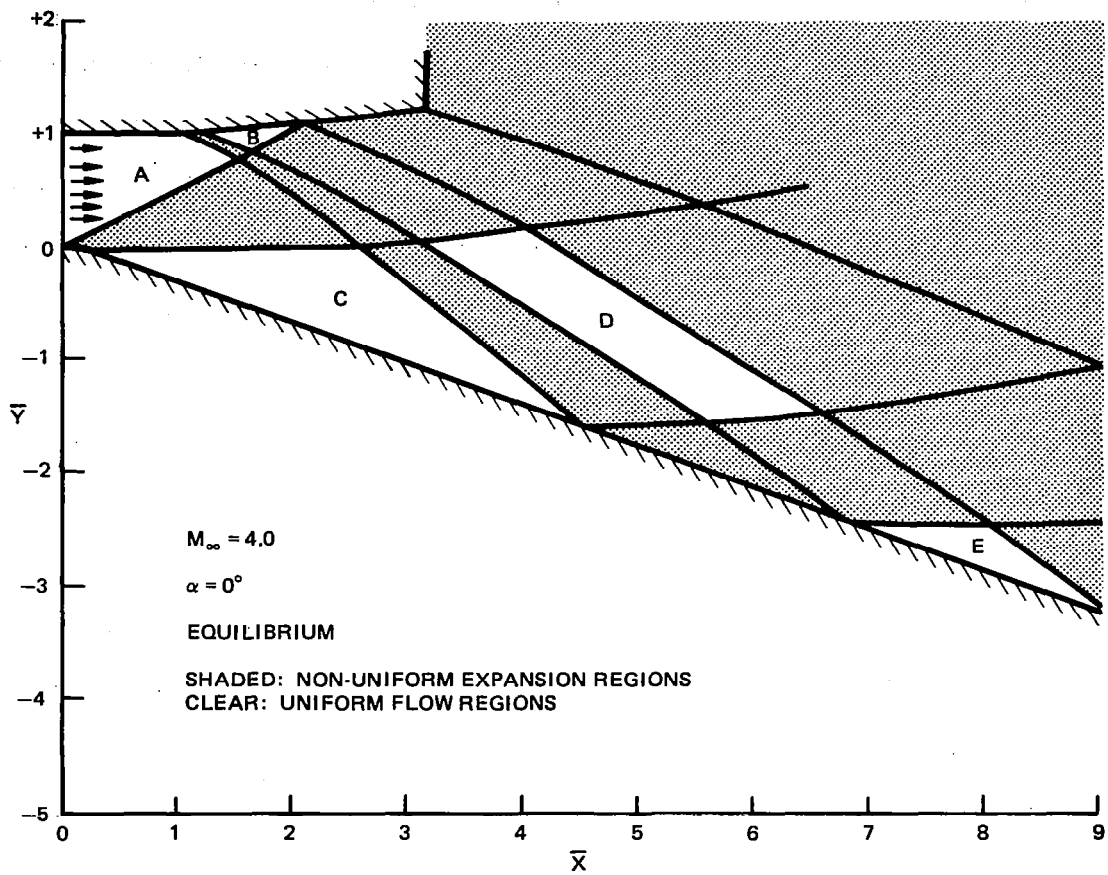

Fig. 2 $M_\infty = 4$ Nozzle Exhaust Flow Field

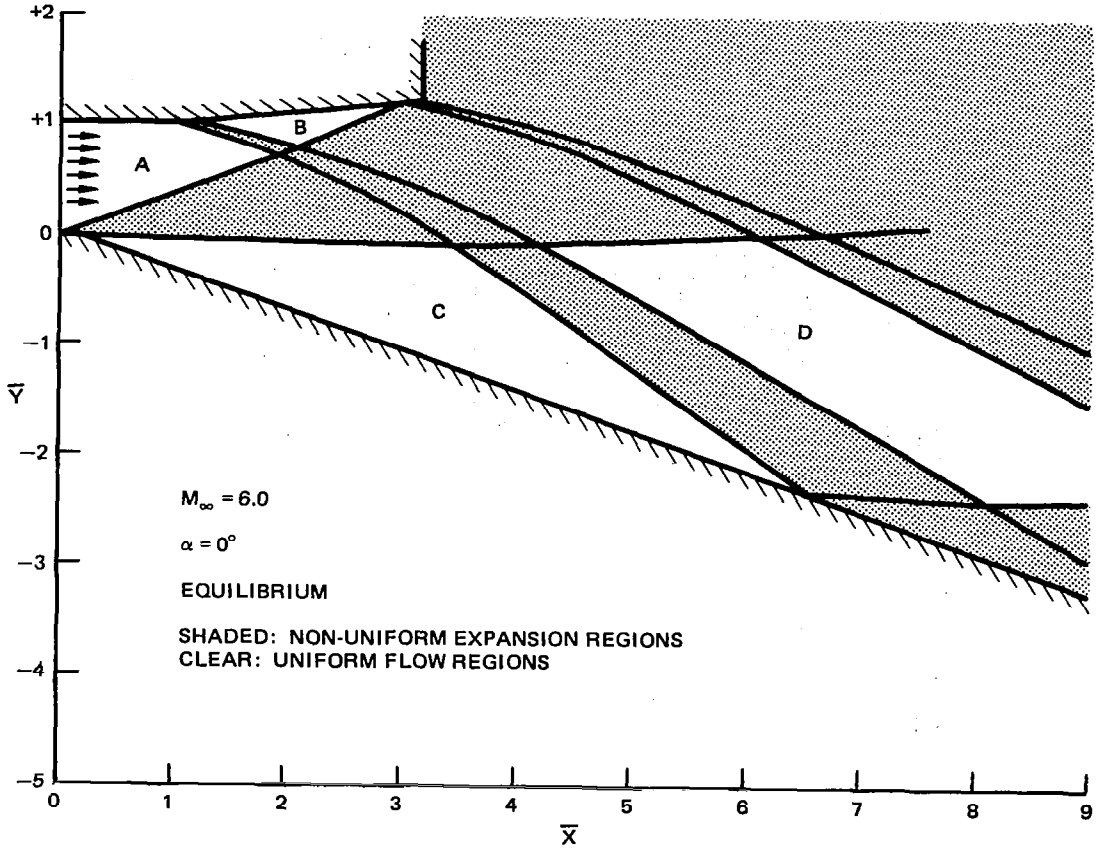

Fig. 3 $M_\infty = 6$ Nozzle Exhaust Flow Field

Table 2 Flow Variables in Flow Field Constant Property Zones

		$M_\infty = 4$ $\alpha = 0°$				$M_\infty = 6$ $\alpha = 0°$			$\alpha = 6°$	
Zone	Property	Real Gas Equilb.	Real Gas Frozen	Best Sub. Gas 60% Ar + 40% $CBrF_3$ T_0 = 533.3 k	Alternate Sub. Gas* 50% Ar + 50% $CBrF_3$ T_0 = 477.8 k	Real Gas Equilb.	Real Gas Frozen	Best Sub. Gas* 50% Ar + 50% $CBrF_3$ T_0 = 477.8 k	Real Gas Equilb.	Real Gas Frozen
A	M	2.129	2.117	2.129	2.129	2.727	2.700	2.727	2.701	2.675
	P/Pe	1.000	1.000	1.000	1.000	1.000	1.000	1.000	1.000	1.000
	θ (deg.)	0.0	0.0	0.0	0.0	0.0	0.0	0.0	0.0	0.0
B	M	2.311	2.307	2.312	2.305	2.931	2.924	2.938	2.905	2.897
	P/Pe	0.7220	0.7207	0.7227	0.7281	0.6745	0.6718	0.6744	0.6766	0.6740
	θ (deg.)	+6.0	+6.0	+6.0	+6.0	+6.0	+6.0	+6.0	+6.0	+6.0
C	M	2.789	2.795	2.782	2.750	3.510	3.527	3.507	3.479	3.494
	P/Pe	0.3073	0.3057	0.3087	0.3186	0.2377	0.2351	0.2381	0.2405	0.2379
	θ (deg.)	-20.0	-20.0	-20.0	-20.0	-20.0	-20.0	-20.0	-20.0	-20.0
D	M	3.023	3.030	3.009	2.962	3.811	3.833	3.798	3.776	3.796
	P/Pe	0.2034	0.2021	0.2045	0.2142	0.1427	0.1408	0.1430	0.1451	0.1431
	θ (deg.)	-14.0	-14.0	-14.0	-14.0	-14.0	-14.0	-14.0	-14.0	-14.0
E	M	3.279	3.288	3.260	3.193	4.146	4.170	4.133	4.110	4.134
	P/Pe	0.1305	0.1294	0.1311	0.1398	0.0824	0.0808	0.0818	0.0839	0.0824
	θ (deg.)	-20.0	-20.0	-20.0	-20.0	-20.0	-20.0	-20.0	-20.0	-20.0

* N.B: Best Substitute gas at $M_\infty = 6$ is the same as $M_\infty = 4$ Alternate Substitute Gas

we chose the case most likely to show a finite-rate chemistry path outside the equilibrium/frozen band to make a one-dimensional-streamtube kinetics calculation using the computer program of Ref. 9. All of the scramjet cases tend toward the frozen situation, but the $M_\infty = 4$ case has lower velocities and higher pressures and temperatures throughout the flow field than the $M_\infty = 6$ case and thus is more likely to have active reactions. In order to exceed the frozen/equilibrium boundaries, the two-body rates must be contributing, while the three-body rates do not. This was most likely to be achieved in the case selected. Two streamtube area distributions were approximated, one very near the 20° afterbody nozzle wall where there is a very rapid initial expansion followed by a long constant-area region, and a second starting at about the middle of the combustor exit plane ($\bar{Y} \simeq 0.46$), where the area remains constant for about one nozzle exit height and then goes through a more gradual expansion. The area distributions used for these two cases are shown in Fig. 4. The combustor exit was assumed to be 15.24 cm (6 in.) high. The results of these calculations showed that there was a negligible difference between the equilibrium, finite-rate, and frozen flows. This is illustrated in Fig. 5 where the pressure distributions for the cases under consideration have been plotted. The other thermodynamic variables behaved similarly. Since two independent computer codes were used for these calculations (Refs. 7 and 9) we made another set of calculations with the Bittker code (Ref. 9) where all the reaction rates were set extremely slow, to simulate a frozen flow. These results were indistinguishable from the frozen flow calculations done with the NASA Lewis Code (Ref. 7), thus validating the consistency of the two codes.

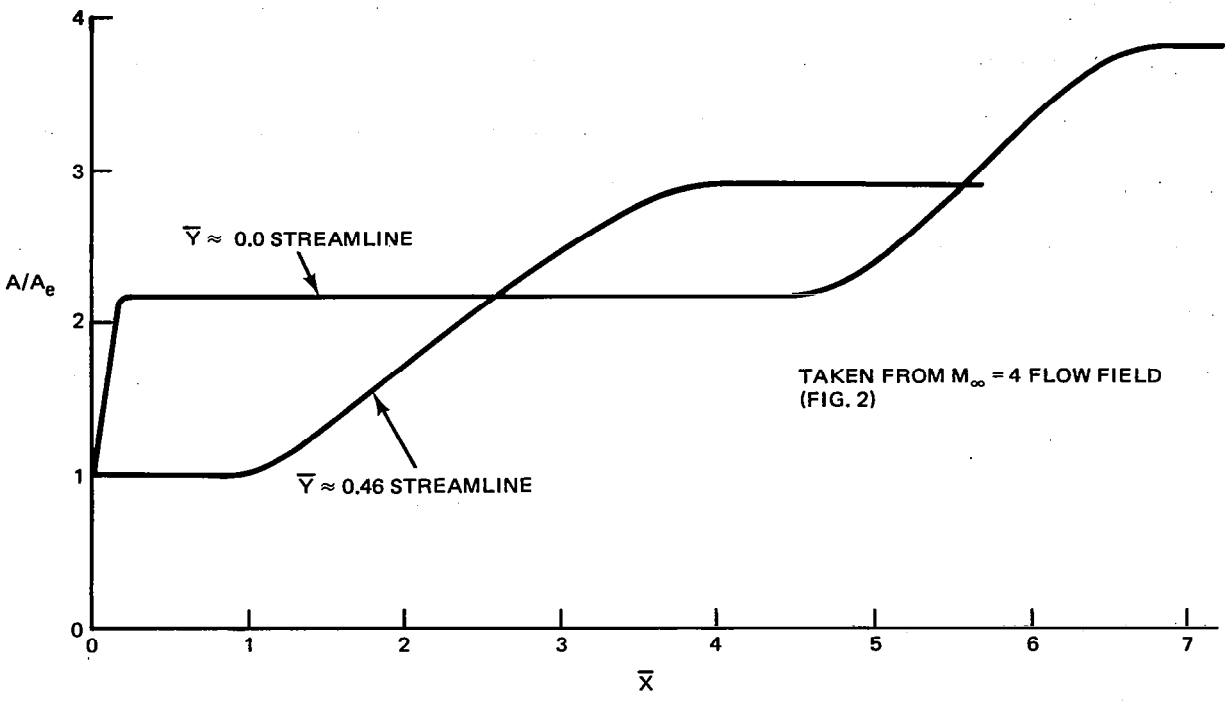

Fig. 4 One-Dimensional Area Ratio Distribution Assumed for Finite-Rate Chemistry Calculation

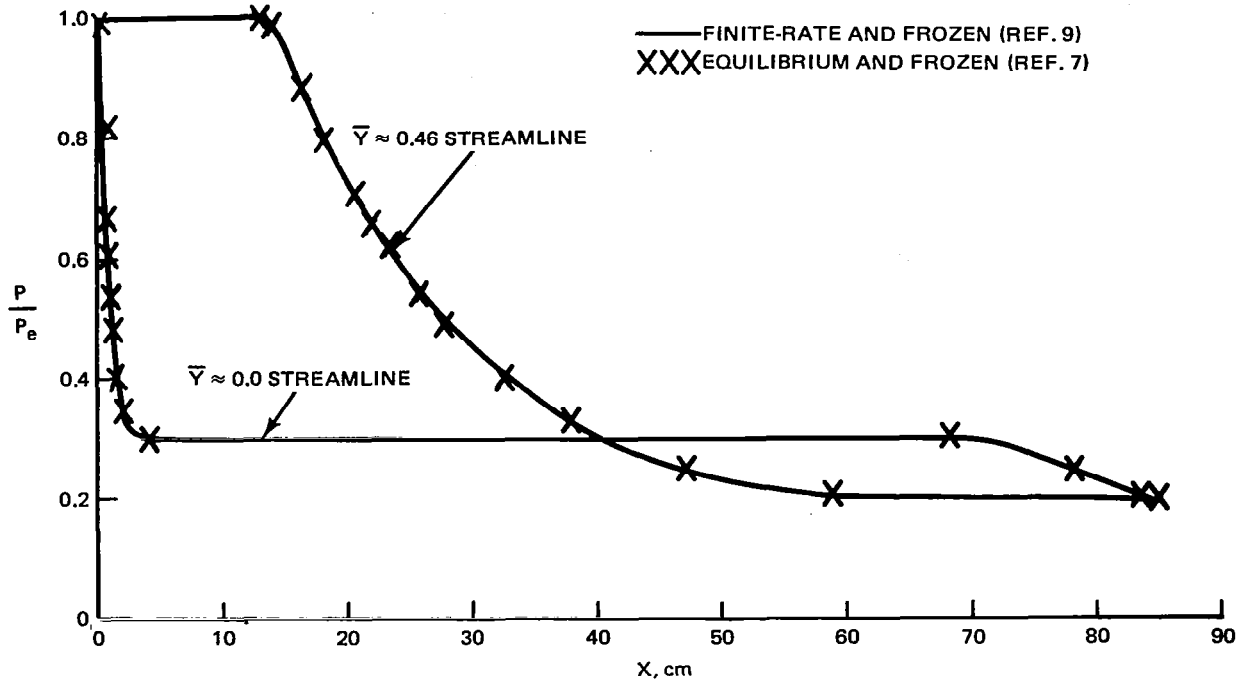

Fig. 5 Pressure Distributions for Two Streamlines in $M_\infty = 4$ Exhaust Flow Field Assuming Equilibrium, Finite-Rate, and Frozen Chemistry

5. INTEGRATED PRESSURE DISTRIBUTIONS

The pressure distributions along the afterbody and cowl surfaces were integrated to compute overall vertical and horizontal forces per unit width, and to serve as the basis for evaluating the various substitute gas mixtures. The vertical force per unit width (F_V) was defined as:

$$F_V = P_e Y_e \int \left(\frac{P}{P_e}\right) \cos\theta \, d\bar{X}$$

and the horizontal force per unit width (F_H) as:

$$F_H = P_e Y_e \int \left(\frac{P}{P_e}\right) \sin\theta \, d\bar{X}$$

In one proposed application of a hydrocarbon fueled scramjet (Ref. 10) the afterbody nozzle is rather short ($\bar{X} < 5$). The present pressure integrations, however, were extended to $\bar{X} = 8$. In order to choose the best substitute gas mixture from the various candidates, we made the judgment that the afterbody pressure distribution should be able to track pressure influences from the cowl. In the $M_\infty = 4$ flight case the presence of the cowl is felt on the afterbody beginning at $\bar{X} \approx 4.5$ (see Fig. 2). In the $M_\infty = 6$ case, however, the cowl influence on the afterbody is delayed to $\bar{X} \tilde{=} 6.5$ (Fig. 3). Thus it became necessary to extend the length of the pressure integration to include effects of the cowl. To illustrate the effect of assuming any particular length afterbody, Fig. 6 shows the running (cumulative), non-dimemsional, vertical forces on the afterbody, as a function of axial distance, for the two flight conditions of interest. Note that this figure also shows the results of some of our substitute gas calculations, which will be discussed in the next Section.

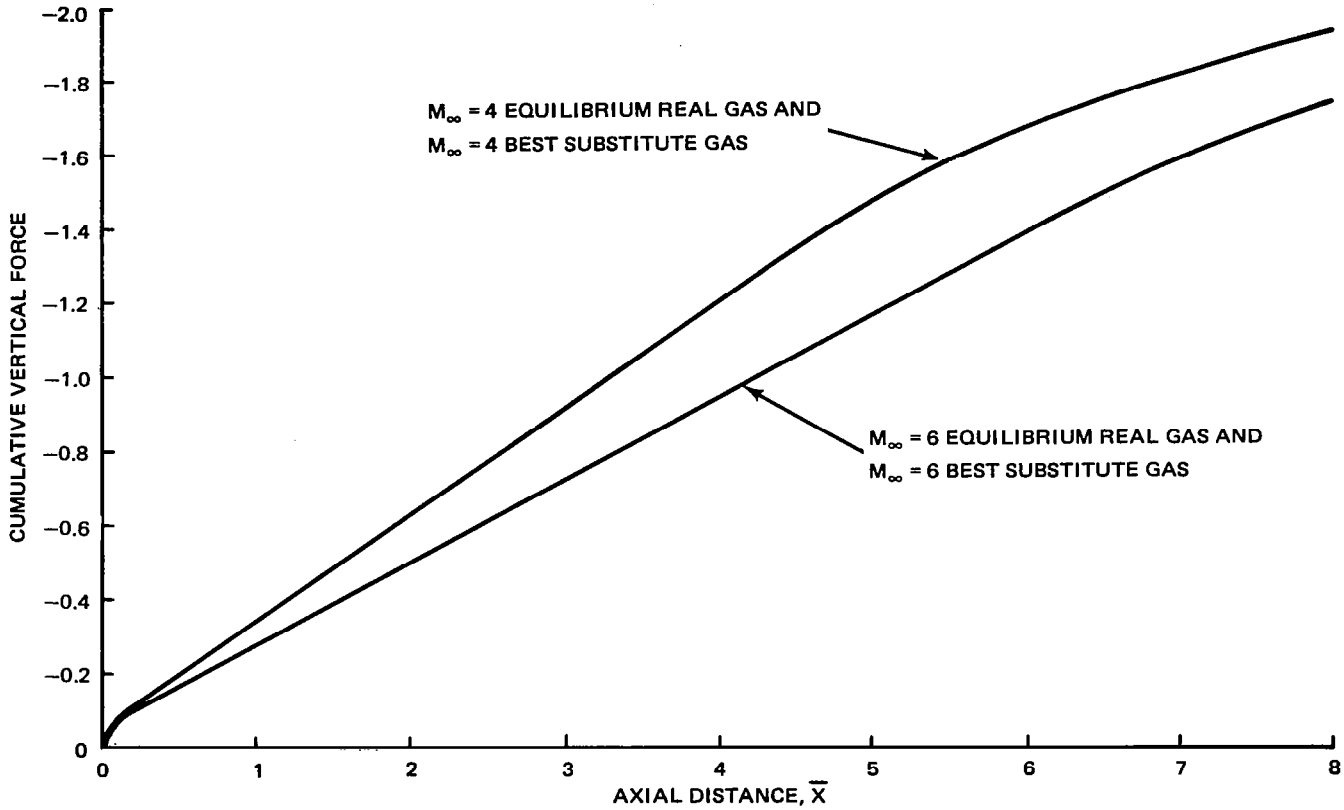

Fig. 6 Non-Dimensional Cumulative Vertical Force on Afterbody

The results of the integrations (normalized by the combustor exit plane pressure and the combustor exit plane height) are shown in Table 3. Note the negligible difference between the frozen and equilibrium flow calculations at each Mach number, and also the negligible effect of angle-of attack at M_∞ = 6. Also shown in this Table (for ease of comparison) are the results from some of the substitute gas calculations (see next Section).

6. SUBSTITUTE GASES

The term "substitute gas" refers to a gas which behaves fluid dynamically and thermodynamically similar to the real gas involved, but is chemically quite different. To simulate the exhaust flow of a hydrocarbon burning scramjet with a real gas would require achieving combustion stagnation temperatures close to 3000 K at stagnation pressures of tens of atmospheres (depending upon the Reynolds number desired) with highly reactive exhaust gases. Such flows are beyond the state of the art of conventional, steady state wind tunnels. The problem can be circumvented by the use of an appropriate substitute gas. This approach to wind tunnel simulation has been validated previously, both experimentally and theoretically (Refs. 3,4,5). The substitute gases used in those examples and proposed for use herein are binary mixtures of argon and fluorocarbons (Freons), mixed in such a ratio and heated to such a stagnation temperature that the flowing gas has the same thermodynamic and fluid dynamic behavior in the flow regime of interest as the real gas. The distinct advantages of the substitute gases are that they require stagnation temperatures of only a few hundred degrees Kelvin and that they are chemically stable and non-reactive.

Table 3 Nozzle Forces from Integrated Pressure Distributions for Hydrocarbon Fuels and Substitute Gases

M_∞	α (deg.)	GAS	COWL	AFTERBODY	NET (Cowl + Afterbody)
			NON-DIMENSIONAL VERTICAL FORCE (F_V/P_eY_e)		
4.0	0.0	Real Equilibrium	2.3134	-1.9419	0.3715
		Real Frozen	2.3053	-1.9311	0.3742
		Best Substitute 60% Ar + 40% $CBrF_3$ T_o = 533.3 K	2.3154	-1.9465	0.3689
		Alternate Sub. 50% Ar + 50% $CBrF_3$ T_o = 477.8 K	2.3291	-2.0057	0.3234
6.0	0.0	Real Equilibrium	2.4548	-1.7517	0.7031
		Real Frozen	2.4458	-1.7342	0.7116
		Best Substitute 50% Ar + 50% $CBrF_3$ T_o = 477.8 K	2.4554	-1.7539	0.7015
	6.0	Real Equilibrium	2.4537	-1.7624	0.6913
			NON-DIMENSIONAL HORIZONTAL FORCE (F_H/P_eY_e)		
4.0	0.0	Real Equilibrium	0.1189	0.6862	0.8051
		Real Frozen	0.1181	0.6823	0.8004
		Best Substitute 60% Ar + 40% $CBrF_3$ T_o = 533.3 K	0.1191	0.6878	0.8069
		Alternate Sub. 50% Ar + 50% $CBrF_3$ T_o = 477.8 K	0.1196	0.7092	0.8288
6.0	0.0	Real Equilibrium	0.1340	0.6181	0.7521
		Real Frozen	0.1331	0.6117	0.7448
		Best Substitute 50% Ar + 50% $CBrF_3$	0.1341	0.6189	0.7530
	6.0	Real Equilibrium	0.1339	0.6219	0.7558

The selection of the proper substitute gas for a particular simulation is basically a trial-and-error procedure. First the desired flow field for the real gas case is calculated (as described in the previous section). Then the calculation is repeated with different substitute gas mixtures at different stagnation temperatures until one combination of mixture-ratio and stagnation temperature match the real gas flow field in a prescribed way. In the present application proper simulation of the surface pressure forces is of major importance and this parameter has been used as the primary criterion to evaluate the candidate substitute gases. In other applications (internal flows, for example), the Mach number or the location of shock waves might be the primary criterion. Since we are dealing with thermally perfect gases, if the initial Mach number and the γ vs. T variation in the flow regime of interest are the same for both the substitute gas mixture and the real gas, then all the other flow parameters will be properly simulated (Ref. 3). Other criteria also to be considered are cost (some fluorocarbons are much more expensive than others), and the required stagnation temperature (obviously the less heating required, the less complexity there will be in the operation of the wind tunnel and its associated equipment).

There is a multitude of substitute gas mixtures and temperatures which could be considered for a particular application. Reference 11 lists the thermodynamic properties of ten different fluorocarbons, several of which, in some combination with argon and at some specified stagnation temperature, might satisfy a particular problem. In an earlier study on the simulation of hydrogen fueled scramjets (Ref. 5) we had calculated the thermodynamic

properties of several substitute gas mixtures. These calculations were applied to the present problem (simulation of hydrocarbon fueled scramjets) and two of the mixtures were found to give excellent simulations of the two basic flight conditions being examined (namely M_∞ = 4.0 @ 6.1 km altitude and M_∞ = 6.0 @ 30.5 km altitude). The best simulation of the Mach 4 flight case was achieved with a mixture of 60% Argon + 40% Freon 13B1 at a stagnation temperature of 533.3 K. The integrated pressure distributions (forces) were different from the equilibrum real gas case only in the 4th significant figure (see Table 3) and the flow fields (e.g. Fig. 2) were indistinguishable. (Note that in Section 3, on Afterbody Nozzle Flow Fields, we concluded that there were negligible differences between equilibrum and frozen flow cases and also between the angle of attack cases. Consequently we made all the substitute gas comparisons just to the equilibrium calculations at zero angle of attack.) Another mixture (50% Argon + 50% Freon 13B1 at a stagnation temperature of 477.8 K) also gave a good simulation of the Mach 4 flight case, the cowl force being about 1/2% too high and the afterbody force about 3% too high. Note that in this case the net vertical force, which is the difference between two relatively large forces, is about 13% different from the desired value. This serves to illustrate how good a simulation was achieved with the substitute gas mixture labeled "best", where the net vertical difference was less than 1% in error. However, the lower stagnation temperature of the alternate gas mixture might make it a more desirable testing medium if component pressures can be measured. We found, for a particular gas mixture in the temperature range examined, that a 55.5 K increase in stagnation temperature produced about a 1% increase in the surface pressures, but since the specific heat ratios (γ) of these mixtures are non-linear with

temperature (see Fig. 1, Ref. 3) we would be cautious about linearly extrapolating one substitute gas mixture performance to other stagnation temperatures.

The "alternate" Mach 4 substitute gas mixture (50% Argon + 50% Freon 13B1 at a stagnation temperature of 477.8 K) proved to give an excellent simulation for the Mach 6 flight case, the integrated pressures again differing only in the 4th significant figure from the equilibrium real gas case (see Table 3). This gas mixture is labeled "best" for the Mach 6 case. The degree to which these "best" substitute gases simulate the real gases is illustrated in Fig. 6 where the cumulative forces on the afterbody are shown to be indistinguishable in each particular case.

It is fortuitous (and fortunate) that this one substitute gas mixture (50% Argon + 50% Freon 13B1 @ T_0 = 477.8 K) should adequately simulate two widely varying flight conditions and flow fields. It should be noted, however, that these two flight conditions have two different combustor exit Mach numbers (see Table 1) and that different supersonic nozzles would have to be used to achieve the proper simulation.

Tables 4 and 5 list the thermodynamic properties of the two substitute gas mixtures just cited.

7. CONCLUSIONS

The afterbody nozzle flow fields for a hydrocarbon burning scramjet have been calculated. Flight conditions of M_∞ =4 @ 6.1 km altitude with α = 0° and M_∞ =6 @ 30.5 km altitude (α = 0° and 6°) were considered. The calculations included equilibrium, frozen and finite-rate chemistry effects.

Table 4 Thermodynamic Properties of 60% Argon + 40% Freon 13B1 Substitute Gas Mixture at T_o = 533.3 K (from Ref. 5)

Mach Number	γ	T(K)	Cp($\frac{cal}{gm\ K}$)	P/Po
5.1299	1.4003	111.1	0.083216	7.9151E-04
4.6384	1.3716	133.3	0.087802	1.5238E-03
4.3317	1.3534	150.0	0.091092	2.3726E-03
4.0626	1.3376	167.7	0.094257	3.5765E-03
3.7473	1.3193	188.9	0.098282	5.9346E-03
3.5357	1.3074	205.6	0.10116	8.4590E-03
3.2786	1.2936	227.8	0.10481	1.3192E-02
3.0436	1.2816	250.0	0.10825	2.0014E-02
2.7732	1.2689	277.8	0.11226	3.2614E-02
2.5215	1.2581	305.6	0.11596	5.1520E-02
2.2361	1.2472	338.9	0.12003	8.6106E-02
2.0062	1.2395	366.7	0.12311	0.12879
1.9152	1.2367	377.8	0.12427	0.15042
1.8242	1.2341	388.9	0.12538	0.17513
1.7329	1.2317	400.0	0.12646	0.20330
1.6870	1.2305	405.6	0.12698	0.21880
1.5945	1.2282	416.7	0.12800	0.25291
1.5006	1.2261	427.8	0.12899	0.29154
1.4048	1.2241	438.9	0.12994	0.33521
1.3062	1.2222	450.0	0.13085	0.38444
1.1511	1.2195	466.7	0.13216	0.47005
1.0407	1.2178	477.8	0.13299	0.53592
0.9827	1.2170	483.3	0.13340	0.57176
0.7190	1.2140	505.6	0.13495	0.73677
0.4487	1.2119	522.2	0.13604	0.88628
0.0000	1.2106	533.3	0.13674	1.00000

Table 5 Thermodynamic Properties of 50% Argon + 50% Freon 13B1 Substitute Gas Mixture at T_o = 477.8 K (from Ref. 5)

Mach Number	γ	T(K)	$Cp(\frac{cal}{gm\ K})$	P/Po
5.0403	1.3695	111.1	0.07799	7.3299E-04
4.5515	1.3378	133.3	0.08333	1.4737E-03
4.0574	1.3072	161.1	0.08955	3.2047E-03
3.6462	1.2833	188.9	0.09531	6.4432E-03
3.2893	1.2644	216.7	0.1006	1.2202E-02
2.9692	1.2490	244.4	0.1055	2.2032E-02
2.6743	1.2364	272.2	0.1101	3.8238E-02
2.3959	1.2258	300.0	0.1142	6.4176E-02
2.1802	1.2186	322.2	0.1173	9.5084E-02
2.0203	1.2137	338.9	0.1195	0.12628
1.8602	1.2093	355.6	0.1216	0.16626
1.7525	1.2066	366.7	0.1229	0.19879
1.6981	1.2053	372.2	0.1235	0.21709
1.6433	1.2041	377.8	0.1242	0.23687
1.5319	1.2017	388.9	0.1254	0.28129
1.4172	1.1994	400.0	0.1268	0.33298
1.2980	1.1972	411.1	0.1277	0.39293
1.1066	1.1942	427.8	0.1294	0.50090
0.9661	1.1924	438.9	0.1304	0.58681
0.8084	1.1906	450.0	0.1314	0.68558
0.6201	1.1890	461.1	0.1324	0.79885
0.3547	1.1874	472.2	0.1333	0.92845
0.0000	1.1866	477.8	0.1338	1.00000

Several candidate substitute gas mixtures were examined for their suitability to simulate the various nozzle flow fields. We found that there were negligible differences in the flow fields between the equilibrium, frozen, and finite rate chemistry assumptions. We also found that increasing the angle-of-attack produced insignificant flow field changes other than raising the overall pressure level. A substitute gas mixture consisting of 60% Argon + 40% Freon 13B1 at a stagnation temperature of 533.3 K gave an excellent simulation of the afterbody flow field for the $M_\infty = 4$ flight case. A substitute gas mixture of 50% Argon + 50% Freon 13B1 at a stagnation temperature of 477.8 K was found to give an excellent simuation for the $M_\infty = 6$ flight case. The latter substitute gas also produced a reasonable simulation for the $M_\infty = 4$ flight case and consequently would appear to be a good candidate for any proposed wind tunnel testing.

8. REFERENCES

1. Weidner, J.P., Small, W.J., and Penland, J.A., "Scramjet Integration on Hypersonic Research Airplane Concepts," Journal of Aircraft, Vol. 14, No. 5, May 1977, pp. 460-466.

2. Hunt, J.L., Lawing, P.L., Marcum, D.C., and Cubbage, J.M., "Performance Potential and Research Needs of a Hypersonic, Airbreathing, Lifting Missile Concept," Journal of Aircraft, Vol. 16, No. 10, October 1979, pp. 666-673.

3. Oman, R.A., Foreman, K.M. Leng, J. and Hopkins, H.B. "Simulation of Hypersonic Scramjet Exhaust." NASA CR-2494, 1975.

4. Hopkins, H.B., Konopka, W., and Leng, J., "Validation of Scramjet Exhaust Simulation Technique," NASA CR-2688, 1976.

5. Hopkins, H.B., Konopka, W., and Leng, J., "Validation of Scramjet Exhaust Simulation Technique at Mach 6," NASA CR-3003, 1979.

6. Burdette, G.W., Lander, H.R., and McCoy, J.R., "High-Energy Fuels for Cruise Missiles," Journal of Energy, Vol. 2, No. 5, Sept-Oct 1978, pp. 289-292.

7. Svehla, R. and McBride, B., "FORTRAN IV Computer Program for Calculation of Thermodynamic and Transport Properties of Complex Chemical Systems," NASA TN D-7056, 1973.

8. Ratliff, A., Smith, S., and Penny, M., "Rocket Exhaust Plume Computer Program Improvement, Vol. 1 - Final Report, Summary Volume, Method-of-Characteristics Nozzle and Plume Programs, "NASA CR-125601, NASA STAR N72-18942, January 1972.

9. Bittker, D.A., and Scullin, V.J. "General Chemical Kinetics Computer Program for Static and Flow Reactions, With Application to Combustion and Shock-Tube Kinetics," NASA TN D-6586, 1972.

10. Hunt, J.L., Johnston, P.J., Cubbage, J.M., Marcum, D.C.,Jr., and Carlson, C.H., "A Mach 6, Airbreathing Surface-to-Air Missile (HYSAM)" (U), Proceedings of 1980 JANNAF Propulsion Meeting, CPIA Publication 315, Vol. II, March 1980, pp. 321-385 (Report Confidential).

11. Talcott, N.A., Jr., "Thermodynamic Properties of Gaseous Fluorocarbons and Isentropic Equilibrium Expansions of Two Binary Mixtures of Fluorocarbons and Argon," NASA TN D-8405, 1977.

1. Report No.	2. Government Accession No.	3. Recipient's Catalog No.
NASA CR-3583		

4. Title and Subtitle	5. Report Date
SIMULATION OF A HYDROCARBON FUELED SCRAMJET EXHAUST	June 1982
	6. Performing Organization Code

7. Author(s)	8. Performing Organization Report No.
Jarvis Leng	RM-743
	10. Work Unit No.

9. Performing Organization Name and Address	11. Contract or Grant No.
Grumman Aerospace Corporation Bethpage, New York 11714	NAS1-16401
	13. Type of Report and Period Covered

12. Sponsoring Agency Name and Address	13. Type of Report and Period Covered
National Aeronautics and Space Administration Washington, DC 20546	Contractor Report
	14. Sponsoring Agency Code

15. Supplementary Notes

Langley Technical Monitor: James L. Hunt
Final Report

16. Abstract

Exhaust nozzle flow fields for a fully integrated, hydrocarbon burning scramjet have been calculated for flight conditions of $M_\infty = 4$ @ 6.1 km altitude and $M_\infty = 6$ @ 30.5 km altitude. Equilibrium flow, frozen flow, and finite-rate chemistry effects were considered. All flow fields were calculated by method-of-characteristics. Finite-rate chemistry results were evaluated by a one-dimensional code (Bittker) using streamtube area distributions extracted from the equilibrium flow field, and compared to very slow artificial rate cases for the same streamtube area distribution. Several candidate substitute gas mixtures, designed to simulate the gas dynamics of the real engine exhaust flow, were examined. Two mixtures were found to give excellent simulations of the specified exhaust flow fields when evaluated by the same method-of-characteristics computer code.

17. Key Words (Suggested by Author(s))	18. Distribution Statement
Engine/Airframe Integration Hydrocarbon Fuel Hypersonic Scramjet Simulation	Unclassified - Unlimited Subject Category 02

19. Security Classif. (of this report)	20. Security Classif. (of this page)	21. No. of Pages	22. Price
Unclassified	Unclassified	31	A03

For sale by the National Technical Information Service, Springfield, Virginia 22161

NASA-Langley, 1982